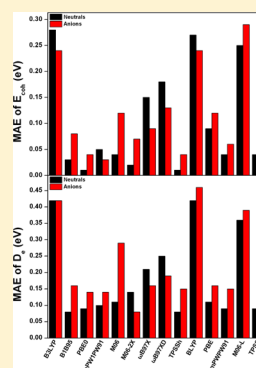


Density Functional Theory Assessment of Molecular Structures and Energies of Neutral and Anionic Al_n ($n = 2-10$) ClustersSelvarengan Paranthaman,^{†,‡} Kiryong Hong,[†] Joonghan Kim,^{*,§} Dong Eon Kim,^{‡,||} and Tae Kyu Kim^{*,†}[†]Department of Chemistry and Chemical Institute for Functional Materials, Pusan National University, Busan 609-735, Republic of Korea[‡]Max Planck Center for Attosecond Science, Pohang 790-784, Republic of Korea[§]Department of Chemistry, The Catholic University of Korea, Bucheon 420-743, Republic of Korea^{||}Department of Physics and Center for Attosecond Science and Technology, POSTECH, Pohang 790-784, Republic of Korea

S Supporting Information

ABSTRACT: We report the results of a benchmarking study on hybrid, hybrid-meta, long-range-corrected, meta-generalized gradient approximation (meta-GGA), and GGA density functional theory (DFT) methods for aluminum (Al) clusters. A range of DFT functionals, such as B3LYP, B1B95, PBE0, mPW1PW91, M06, M06-2X, ω B97X, ω B97XD, TPSSh, BLYP, PBE, mPWPW91, M06-L, and TPSS, have been used to optimize the molecular structures and calculate the vibrational frequencies and four energetic parameters for neutral and anionic Al_n ($n = 2-10$) clusters. The performances of these functionals are assessed systematically by calculating the vertical ionization energy for neutral Al clusters and the vertical electron detachment energy for anionic Al clusters, along with the cohesive energy and dissociation energy. The results are compared with the available experimental and high-level ab initio calculated results. The calculated results showed that the PBE0 and mPW1PW91 functionals generally provide better results than the other functionals studied. TPSS can be a good choice for the calculations of very large Al clusters. On the other hand, the B3LYP, BLYP, and M06-L functionals are in poor agreement with the available experimental and theoretical results. The calculated results suggest that the hybrid DFT functionals like B3LYP do not always provide better performance than GGA functionals.



■ INTRODUCTION

Aluminum clusters have attracted considerable interest because of their potential applications in high energy density materials^{1,2} and catalysis.^{3,4} Over the past two decades, extensive theoretical⁵⁻¹⁴ and experimental^{14,10,15-18} studies of Al clusters have been performed with particular focus on their structural, electronic, optical, and magnetic properties. Because the reactivity of metal clusters strongly depends on their energetic properties, such as ionization potential and electron affinity, a reasonably accurate and efficient theoretical method to calculate the properties will be needed to predict the reactivity of metal clusters. In this regard, density functional theory (DFT) has been a good choice because of its relatively shorter computation time than those of the post-Hartree–Fock, wave function based methods. The performance of DFT depends not only on choosing exchange–correlation functionals but also on correctly choosing reasonable-sized basis sets for the study. The effect of basis set on Al clusters was previously reported by researchers.¹⁹⁻²¹ On the other hand, a few DFT assessment studies have also been performed on Al clusters.²¹⁻²³ For example, Drebov and Ahlrichs²³ have studied neutral Al clusters using coupled-cluster singles and doubles including perturbative corrections for triple excitations [CCSD(T)] and four DFT functionals (PBE, TPSS, BP86, and B3LYP). Their calculated results showed that the PBE (general gradient approximation,

GGA) and B3LYP (hybrid) functionals were in poor agreement with the available experimental and CCSD(T) results. In particular, B3LYP has the largest maximum absolute deviation of the dissociation energy (D_e) from the CCSD(T) results. In contrast, TPSS, which is a meta-GGA functional, showed the smallest maximum absolute deviation of D_e . Therefore, TPSS was the best functional among those studied. These results are unexpected because B3LYP is one of the most widely used DFT functionals for studying Al clusters.²⁴⁻²⁸ Nevertheless, these studies did not assess the most important energetic parameters, such as ionization energy and electron affinity of various anionic and neutral Al clusters. To the best of our knowledge, there has been no systematic assessment of Al clusters using a large number of recently developed hybrid, hybrid-meta, and long-range-corrected DFT functionals.

For this purpose, neutral and anionic Al_n ($n = 2-10$) clusters are investigated systematically with a range of DFT functionals, with particular focus on the recently developed DFT functionals. The main purpose is to understand the difference in performance of various recently developed DFT functionals along with the most frequently used DFT functionals, and to

Received: July 26, 2013

Revised: August 27, 2013

Published: September 13, 2013

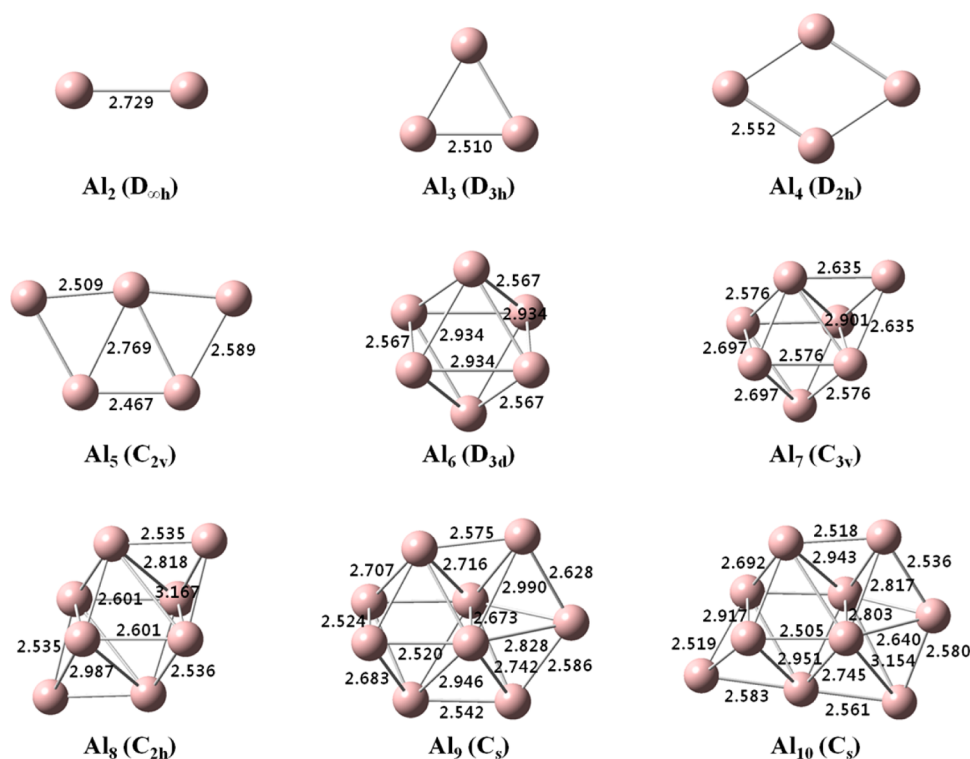


Figure 1. Optimized structures (distances in angstroms) of neutral Al_n ($n = 2-10$) clusters by PBE0/def2-TZVPP.

find a suitable DFT functional with accuracy reasonably close to high-level ab initio methods, such as CCSD(T). Because the CCSD(T) method provides good results compared to the available experimental results, the experimental results are partially replaced with the CCSD(T) results for cases where experimental results are unavailable. Energetic parameters, such as vertical ionization energy (vIE) for neutral clusters and vertical electron detachment energy (vEDE, electron affinity) for anion clusters, as well as the cohesive energy (E_{coh}) and dissociation energy (D_e) were calculated to select the optimal DFT functionals for Al_n clusters. The latter two parameters in a previous study were considered to assess the DFT functionals.²³ Two energetic parameters (vIE and vEDE) are also included, making an assessment of the DFT performance more reasonable. The present study examined DFT performance by calculating the four energetic parameters of Al clusters. This work is expected to assist in the selection of suitable DFT functionals for further investigations of large-sized Al clusters and quantum mechanics/molecular dynamics (QM/MD) simulations for the catalytic reaction of Al clusters.

COMPUTATIONAL DETAILS

Molecular structures of neutral and anionic Al clusters were optimized by use of the following range: DFT methods, B3LYP,^{29,30} B1B95,^{29,31} PBE0,³² mPW1PW91,^{33,34} M06,³⁵ M06-2X,³⁵ ω B97X,³⁶ ω B97XD,³⁷ TPSSH,³⁸ BLYP,^{29,30} PBE,^{39,40} mPWPW91,^{33,34} M06-L,⁴¹ and TPSS.⁴² Second-generation default bases and triple- ζ valence with heavily polarized basis functions (def2-TZVPP)⁴³ were used. The reliability of the def2-TZVPP basis set ((14s 9p 3d 1f)/[5s 5p 3d 1f]) was tested in an earlier study on Al clusters.²³ One of the main purposes of the present study is to identify a suitable DFT functional for further investigations of large Al clusters. For this, the segment contraction basis set in the DFT

calculations is more appropriate than a general contraction one, such as the correlation-consistent (CC) basis set. Therefore, the cc-pVXZ ($X = \text{T or Q}$) basis set was not used. In addition, CCSD(T)⁴⁴ calculations were performed with the def2-QZVPP basis set⁴³ for neutral and anionic clusters due to the lack of experimental results for these clusters. Geometry optimizations using CCSD(T) were performed only for Al_2 – Al_4 clusters. On the other hand, CCSD(T) single-point energy calculations were performed on the optimized geometries by PBE0/def2-TZVPP in the cases of Al_5 – Al_{10} clusters.⁴³ Spin-restricted and unrestricted formalisms were used to calculate the singlet and doublet spin states, respectively. The molecular structures were fully optimized within the specified molecular symmetry. For geometry optimizations, initial structures of the neutral Al clusters were obtained from the literature.²³ After geometry optimizations of the neutral Al clusters were performed, their optimized structures were used as the initial structures of the anionic Al clusters. Vibrational frequency calculations were performed for all neutral and anionic Al clusters to identify the minimum energy structure. In addition, the vIE of neutral Al clusters and the vEDE of anionic Al clusters, along with E_{coh} and D_e , were calculated. In addition, it must be noted that earlier studies^{9,45} have mentioned that the favorable dissociation channel of Al_n^- is Al_{n-1}^- and Al. All vIE and vEDE were obtained with a zero-point energy (ZPE) correction. The vIE values were calculated by the difference between ground-state energies of neutral and ionized clusters with a neutral geometry:

$$\text{vIE} = E_n^+ - E_n \quad (1)$$

The vEDE values were calculated from the difference in ground-state energies between anionic and neutral clusters with an anion geometry:

$$\text{vEDE} = E_n - E_n^- \quad (2)$$

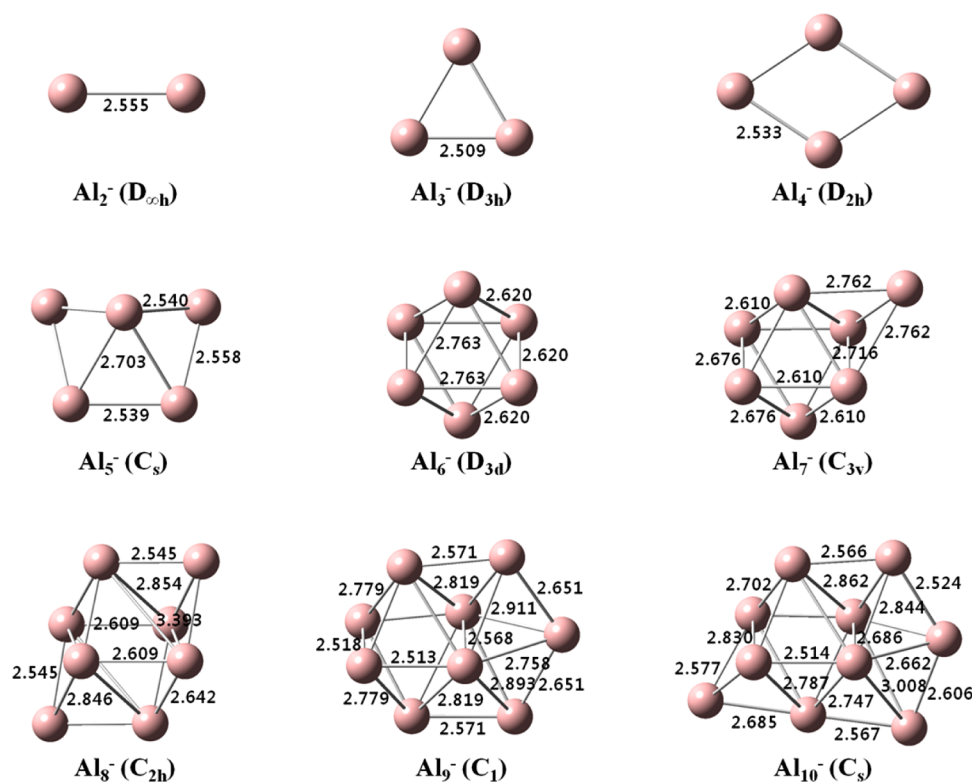


Figure 2. Optimized structures (distances in angstroms) of anionic Al_n^- ($n = 2-10$) clusters by PBE0/def2-TZVPP.

The $E_{\text{coh}}(n)$ values for Al clusters were obtained from eqs 2 and 4:

For neutral clusters:

$$E_{\text{coh}}(n) = \frac{nE(\text{Al}) - E(\text{Al}_n)}{n} \quad (3)$$

For anion clusters:

$$E_{\text{coh}}(n) = \frac{(n-1)E(\text{Al}) + E(\text{Al}^-) - E(\text{Al}_n^-)}{n} \quad (4)$$

The $D_e(n)$ values for Al clusters were obtained from eq 5:

$$D_e(n) = E(\text{Al}) + E(\text{Al}_{n-1}^x) - E(\text{Al}_n^x) \quad (5)$$

where n represents the number of atoms, E represents the total energy of atom or clusters, and $x = 0$ for neutral clusters and $x = -1$ for anion clusters. All calculations were performed by use of the Gaussian09 program.⁴⁶

RESULTS AND DISCUSSION

Cluster Structures. Optimized structures of neutral and anionic Al clusters are shown in Figures 1 and 2, respectively. In the case of neutral clusters, the B1B9S, PBE0, mPW1PW91, TPSSH, PBE, mPWPW91, and TPSS functionals predict all the clusters within their symmetry, which were found by Drebov and Ahlrichs²³ On the other hand, other functionals provide the structures with a small imaginary frequency in some cases. For example, both M06 and M06-L functionals predict the C_1 structure as the minimum energy structure of Al_5 in this study instead of the C_{2v} structure predicted by Drebov and Ahlrichs. Furthermore, ωB97X and ωB97XD functionals predict a structure with C_s symmetry as the minimum energy structure of an Al_8 cluster rather than the C_{2h} structure. Accordingly, the symmetry was reduced by removing the imaginary frequency.

For example, the B3LYP functional gives C_s structures, which lie slightly lower in energy than the C_{3v} structure of Al_7 and the C_{2h} structure of Al_8 . The C_{3v} and C_{2h} structures of the Al_7 and Al_8 clusters optimized by B3LYP, respectively, have one imaginary frequency whose magnitude is quite small ($\sim 50 \text{ cm}^{-1}$). The results of the B3LYP functional are consistent with an earlier study by Sun et al.,²⁵ who predicted that the C_s structures optimized by use of B3LYP/6-311G(2d) are the minimum-energy structures of Al_7 and Al_8 clusters. In the case of anionic clusters, the M06-L, ωB97X , and ωB97XD functionals predict all anionic clusters within their respective symmetry structures of neutral clusters. On the other hand, some other functionals predict structures that have lower symmetry than the neutral clusters. M06 gives one imaginary frequency for the D_{2h} structure of an Al_4^- cluster. In contrast, there is no imaginary frequency on the C_s structure of the Al_4^- cluster. In the case of the Al_5^- cluster, all functionals predicted the C_s structure rather than the C_{2v} structure, which is also predicted in the neutral Al_5 cluster (see Figure 1). This result is also consistent with those obtained in a recent theoretical study [BPW91/6-311+G(2d)].¹²

The main focus of this study is to assess the performance of the recently developed hybrid, hybrid-meta, and long-range-corrected DFT functionals in examining Al clusters. Therefore, it would be necessary to compare the calculated results with the available experimental data. However, experimental values for the molecular structure and vibrational frequency are available only for neutral Al_2 and anionic Al_3^- .⁴⁷⁻⁴⁹ and vibrational frequencies are available only for Al_3 .^{49,50} As mentioned above, the results calculated by CCSD(T)/def2-QZVPP, which is sufficiently high-level theory, are used as reference values if experimental values are unavailable. The optimized geometrical parameters of neutral Al_n ($n = 2-4$) and anionic Al_n^- ($n = 2-4$) clusters are summarized in Tables 1 and 2, respectively. As

Table 1. Optimized Structural Parameters of Neutral Al₂–Al₄ Clusters

param ^a	B3LYP	B1B95	PBE0	mPW1PW91	M06	M06-2X	ω B97X	ω B97XD	TPSSH	BLYP	PBE	mPWPW91	M06-L	TPSS	CCSD(T) ^b	expt
Al₂ Cluster, ³Π_u State ($D_{\infty h}$ Symmetry)																
$r(\text{Al}–\text{Al})$	2.753	2.727	2.729	2.728	2.722	2.726	2.691	2.710	2.730	2.787	2.755	2.755	2.711	2.739	2.713	2.701 ^c
vIE	6.13	6.10	6.29	6.29	6.22	6.30	6.48	6.48	6.51	5.97	6.29	6.30	6.29	6.29	6.29	6.0–6.42 ^d
E_{coh}	0.67	0.73	0.76	0.75	0.75	0.75	0.68	0.68	0.74	0.68	0.81	0.79	0.80	0.76	0.70	
D_e	1.34	1.46	1.53	1.49	1.50	1.49	1.36	1.36	1.49	1.37	1.62	1.58	1.59	1.52	1.41	1.36 ± 0.06 ^{c,e}
Al₂ Cluster, ³Σ_g^- State																
$r(\text{Al}–\text{Al})$	2.502	2.478	2.478	2.478	2.471	2.502	2.461	2.481	2.477	2.52	2.489	2.49	2.448	2.481	2.481	2.467 ^c
D_e	1.22	1.44	1.48	1.44	1.48	1.45	1.13	1.17	1.47	1.30	1.66	1.61	1.69	1.54	1.36	
Al₃ Cluster (D_{3h} Symmetry)																
$r(\text{Al}–\text{Al})$	2.534	2.502	2.510	2.510	2.510	2.520	2.502	2.515	2.508	2.550	2.520	2.521	2.480	2.511	2.523	
vIE	6.66	6.53	6.76	6.78	6.42	6.53	6.66	6.70	6.75	6.32	6.50	6.50	6.46	6.52	6.64	6.42–6.5 ^d
E_{coh}	1.09	1.28	1.27	1.24	1.30	1.28	1.13	1.13	1.27	1.12	1.36	1.32	1.44	1.31	1.26	
D_e	1.92	2.38	2.28	2.22	2.39	2.35	2.03	2.03	2.34	1.99	2.47	2.39	2.74	2.40	2.37	
Al₄ Cluster (D_{2h} Symmetry)																
$r(\text{Al}–\text{Al})$	2.576	2.546	2.552	2.554	2.540	2.562	2.541	2.555	2.551	2.594	2.563	2.564	2.517	2.554	2.562	
vIE	6.55	6.51	6.69	6.70	6.52	6.55	6.54	6.57	6.69	6.24	6.55	6.54	6.54	6.58	6.89	≥6.5 ^d
E_{coh}	1.26	1.48	1.48	1.44	1.50	1.47	1.29	1.29	1.49	1.29	1.59	1.55	1.68	1.53	1.47	
D_e	1.76	2.10	2.11	2.06	2.11	2.03	1.75	1.76	2.14	1.82	2.27	2.21	2.39	2.20	2.09	

^aBond lengths are given in angstroms; vIE, E_{coh} , and D_e values are given in electronvolts. ^bCCSD(T)/def2-QZVPP in ref 23 and vIEs were calculated by use of CCSD(T)/def2-QZVPP/PBE0/def2-TZVPP in this study. ^cReference 48. ^dReference 15. ^eReference 49.

Table 2. Optimized Structural Parameters of Anionic Al_2^- – Al_4^- Clusters

param ^a	B3LYP	B1B95	PBE0	mPW1PW91	M06	M06-2X	ω B97X	ω B97XD	TPSSH	BLYP	PBE	mPWPW91	M06-L	TPSS	CCSD(T) ^b	expt
Al_2^- Cluster ($D_{\infty h}$ Symmetry)																
$r(\text{Al}–\text{Al})$	2.570	2.549	2.555	2.554	2.545	2.544	2.510	2.528	2.556	2.600	2.579	2.579	2.532	2.564	2.555	
$\nu_{\text{E}}(\text{Al}–\text{Al})$	1.32	1.25	1.45	1.47	1.16	1.27	1.41	1.42	1.42	1.10	1.37	1.39	1.30	1.39		1.46 ± 0.01, ^c 1.60 ^d
E_{coh}	1.26	1.37	1.37	1.35	1.41	1.42	1.28	1.27	1.36	1.27	1.43	1.41	1.47	1.38	1.29	
D_{e}	2.54	2.70	2.94	2.91	2.65	2.74	2.55	2.61	2.90	2.41	3.03	3.00	2.99	2.93	2.91	
Al_3^- Cluster (D_{3h} Symmetry)																
$r(\text{Al}–\text{Al})$	2.528	2.498	2.509	2.509	2.519	2.507	2.498	2.502	2.510	2.544	2.519	2.52	2.484	2.514	2.525	2.51 ± 0.02 ^e
$\nu_{\text{E}}(\text{Al}–\text{Al})$	1.50	1.41	1.52	1.53	1.52	1.52	1.48	1.55	1.50	1.35	1.53	1.54	1.45	1.51		1.89 ± 0.04, ^c 1.90, ^d 1.916 ± 0.004 ^f
E_{coh}	1.59	1.78	1.73	1.69	1.88	1.83	1.65	1.64	1.73	1.63	1.84	1.79	1.93	1.77	1.77	
D_{e}	2.27	2.60	2.44	2.38	2.81	2.65	2.39	2.38	2.48	2.34	2.64	2.56	2.85	2.55	2.74	
Al_4^- Cluster (D_{2h} Symmetry)																
$r(\text{Al}–\text{Al})$	2.559	2.524	2.533	2.534	2.524	2.528	2.506	2.524	2.534	2.587	2.55	2.552	2.499	2.54	2.548	
$\nu_{\text{E}}(\text{Al}–\text{Al})$	2.21	2.14	2.38	2.39	1.82	2.17	2.28	2.27	2.36	1.80	1.99	2.00	2.25	2.01		2.20 ± 0.05, ^c 2.20 ^d
E_{coh}	1.75	1.97	1.95	1.91	1.82	1.98	1.81	1.80	1.96	1.78	2.06	2.01	2.17	2.00	1.93	
D_{e}	2.21	2.56	2.62	2.57	1.67	2.43	2.29	2.26	2.66	2.25	2.72	2.66	2.88	2.70	2.40	

^aBond lengths are given in angstroms; $\nu_{\text{E}}(\text{Al}–\text{Al})$, E_{coh} , and D_{e} values are given in electronvolts. ^bValues were optimized by CCSD(T)/def2-QZVPP in this work. ^cReference 54. ^dReference 55. ^eReference 49. ^fReference 57.

can be seen in Tables 1 and 2, the bond lengths of Al_2^- and Al_3^- calculated by CCSD(T)/def2-QZVPP are in excellent agreement with the experimental values. In addition, the bond length of Al_3^- optimized by CCSD(T)/def2-QZVPP (2.523 Å) is very similar to that (2.534 Å) of MRCI/aug-cc-pVQZ.⁵¹ All the results suggest that the values calculated by CCSD(T)/def2-QZVPP can be considered as reference values for further comparisons.

To visualize the performance of the DFT functionals, Figure 3a shows the mean absolute errors (MAE) for Al–Al bond

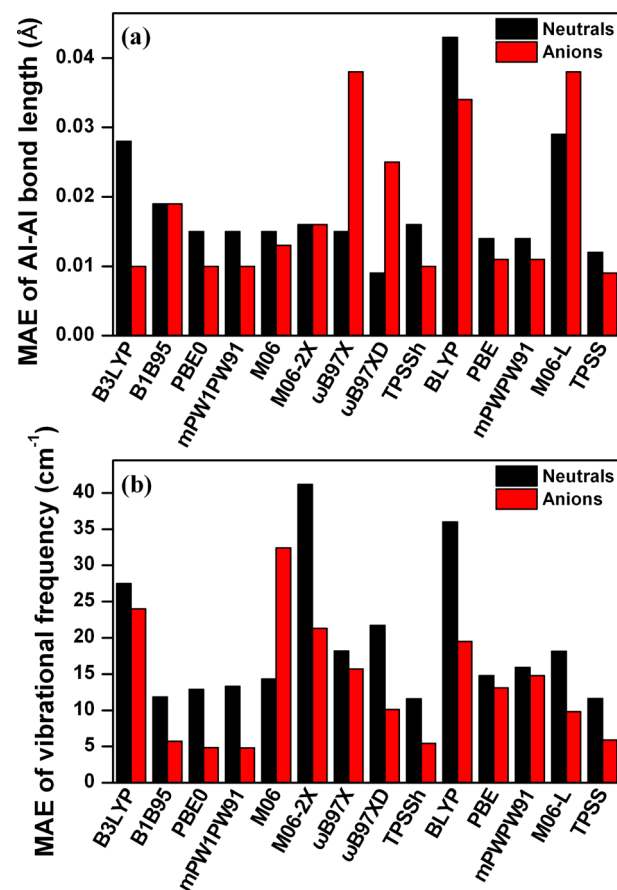


Figure 3. Mean absolute errors of (a) Al–Al bond length and (b) vibrational frequency of Al_2^- – Al_4^- clusters.

length compared to the available experimental and CCSD(T) results. For Al_2^- – Al_4^- clusters, geometry optimizations and subsequent vibrational frequency calculations were performed with CCSD(T)/def2-QZVPP because no experimental values are available. The ground and first excited states of Al_2^- are the $^3\Pi_u$ and $^3\Sigma_g^-$ states, respectively.⁵² All functionals successfully predicted that the $^3\Pi_u$ state is the ground state of Al_2^- . The MAEs of Al–Al bond length for neutral Al_2^- – Al_4^- clusters show that ω B97X and ω B97XD (including empirical dispersion correction), which are recently developed long-range-corrected functionals, have slightly less deviation than the other DFT functionals when compared with the experimental^{47,48} and high-level theoretical values.²³ Including the dispersion correction (in a comparison between ω B97X and ω B97XD results) would result in less deviation in Al–Al bond length. This indicates that the dispersion effect also contributes to the molecular structures of neutral Al clusters. Other hybrid or hybrid-meta DFT functionals such as PBE0, mPW1PW91,

Table 3. Calculated vIE , E_{coh} , and D_e Values for Neutral Al_n ($n = 5-10$) Clusters

cluster (symm)	B3LYP	B1B95	PBE0	mPW1PW91	M06	M06-2X	ω B97X	ω B97XD	TPSSH	BLYP	PBE	mPWPW91	M06-L	TPSS	CCSD(T)	expt ^a
Al_5 (C_{2v})	6.45	6.39	6.63	6.64	6.20 ^b	6.38	6.70	6.65 ^c	6.58	6.20	6.45	6.45	6.40 ^b	6.45	6.54 ^d	6.42–6.5
Al_6 (D_{3d})	6.47	6.56	6.61	6.61	6.57	6.61	6.61	6.60	6.63	6.28	6.59	6.58	6.61	6.62	6.76 ^d	6.0–6.42
Al_7 (C_{3v})	5.85 ^c	5.99	6.14	6.14	5.97	6.05	6.19	6.22	6.14	5.58 ^c	6.06	6.06	5.95	6.11	6.14 ^d	6.0–6.42
Al_8 (C_{2h})	6.08 ^c	6.11	6.24	6.25	6.09	6.15	6.24 ^c	6.20 ^c	6.22	5.90	6.15	6.16	6.09	6.18	6.33 ^d	~6.42
Al_9 (C_3)	6.13	6.19	6.37	6.37	6.20	6.29	6.22	6.31	6.34	5.89	6.15	6.16	6.17	6.12	6.33 ^d	≤6.42
Al_{10} (C_2)	5.85	5.88	5.96	5.96	5.88	5.96	5.92	5.89	5.95	5.65	5.93	5.93	5.86	5.94	6.27 ^d	5.9–6.42
E_{coh} (eV)																
Al_5 (C_{2v})	1.45	1.69	1.70	1.66	1.74 ^b	1.65	1.53	1.52 ^c	1.71	1.48	1.80	1.75	1.91 ^b	1.74	1.69 ^c	1.69 ^c
Al_6 (D_{3d})	1.61	1.97	1.91	1.86	1.99	1.95	1.75	1.72	1.92	1.63	2.02	1.96	2.20	1.96	1.93 ^c	1.93 ^c
Al_7 (C_{3v})	1.79 ^c	2.20	2.15	2.09	2.18	2.15	1.99	1.94	2.15	1.79 ^c	2.23	2.16	2.46	2.18	2.15 ^c	2.15 ^c
Al_8 (C_{2h})	1.80 ^c	2.21	2.16	2.10	2.19	2.15	1.99 ^c	1.94 ^c	2.17	1.80	2.25	2.18	2.47	2.20	2.17 ^c	2.17 ^c
Al_9 (C_3)	1.83	2.28	2.23	2.17	2.28	2.22	2.08	2.02	2.23	1.82	2.31	2.24	2.55	2.26	2.23 ^c	2.23 ^c
Al_{10} (C_2)	1.88	2.33	2.27	2.21	2.31	2.26	2.12	2.06	2.28	1.87	2.36	2.28	2.61	2.31	2.28 ^c	2.28 ^c
D_e (eV)																
Al_5 (C_{2v})	2.24	2.54	2.57	2.52	2.70 ^b	2.40	2.51	2.43 ^c	2.57	2.23	2.63	2.57	2.84 ^b	2.59	2.57 ^c	2.57 ^c
Al_6 (D_{3d})	2.40	3.35	3.00	2.89	3.22	3.44	2.83	2.71	3.00	2.37	3.12	3.00	3.65	3.05	3.15 ^c	3.15 ^c
Al_7 (C_{3v})	2.85 ^c	3.56	3.53	3.45	3.36	3.34	3.43	3.25	3.54	2.73 ^c	3.49	3.39	3.97	3.53	3.43 ^c	3.43 ^c
Al_8 (C_{2h})	1.92 ^c	2.30	2.24	2.18	2.26	2.16	2.03 ^c	1.97 ^c	2.26	1.93	2.39	2.32	2.59	2.32	2.37 ^c	2.37 ^c
Al_9 (C_3)	2.08	2.87	2.78	2.69	2.95	2.81	2.79	2.70	2.77	2.00	2.78	2.67	3.19	2.77	2.66 ^c	2.66 ^c
Al_{10} (C_2)	2.32	2.76	2.71	2.64	2.65	2.55	2.52	2.36	2.72	2.30	2.79	2.72	3.12	2.75	2.79 ^c	2.79 ^c

^aReference 16. ^b C_1 symmetry. ^c C_3 symmetry. ^dValues were calculated by CCSD(T)/def2-QZVPP//PBE0/def2-TZVPP in this work. ^eReference 23.

Table 4. Calculated vEDE, E_{coh} , and D_e Values for Anionic Al_n^- ($n = 5-10$) Clusters

cluster (symm)	B3LYP	B1B95	PBE0	mPW1PW91	M06	M06-2X	ω B97X	ω B97XD	TPSSH	BLYP	PBE	mPWPW91	M06-L	TPSS	CCSD(T) ^a	expt
$\text{Al}_5^- (\text{C}_s)$	1.93	1.88	1.97	1.97	1.98	1.91	1.90	1.95	1.96	1.76	1.98	1.99	1.96	1.97		$2.25 \pm 0.05^b, 2.30^c$
$\text{Al}_6^- (\text{D}_{3d})$	2.37	2.45	2.63	2.62	2.33	2.39	2.60	2.57	2.11	2.11	2.40	2.40	2.55	2.43		$2.63 \pm 0.06^b, 2.65^c$
$\text{Al}_7^- (\text{C}_{3v})$	2.10	2.05	2.13	2.14	2.16	2.19	2.19	2.23	2.11	1.94	2.14	2.14	2.01	2.11		$2.43 \pm 0.06^b, 2.50^c$
$\text{Al}_8^- (\text{C}_{2h})$	1.93	1.82	2.03	2.05	1.89	1.92	1.94	2.01	2.01	1.76	1.99	2.00	1.81	1.99		$2.35 \pm 0.08^b, 2.40^c$
$\text{Al}_9^- (\text{C}_1)$	2.43	2.56	2.67	2.68	2.60	2.79	2.37	2.45	2.47	2.25	2.46	2.46	2.38	2.46		$2.85 \pm 0.08^b, 2.90^c$
$\text{Al}_{10}^- (\text{C}_i)$	2.32	2.33	2.49	2.49	2.37	2.46	2.58	2.61	2.46	2.10	2.40	2.40	2.31	2.42		$2.70 \pm 0.07^b, 2.80^c$
$E_{\text{coh}} (\text{eV})$																
$\text{Al}_5^- (\text{C}_s)$	1.84	2.09	2.07	2.02	2.16	2.09	1.93	1.91	2.07	1.87	2.17	2.12	2.30	2.11	2.04	
$\text{Al}_6^- (\text{D}_{3d})$	1.98	2.37	2.30	2.25	2.39	2.36	2.17	2.12	2.31	1.99	2.40	2.33	2.61	2.35	2.27	
$\text{Al}_7^- (\text{C}_{3v})$	2.07	2.49	2.41	2.35	2.51	2.47	2.29	2.24	2.42	2.06	2.50	2.43	2.73	2.45	2.39	
$\text{Al}_8^- (\text{C}_{2h})$	2.05	2.45	2.40	2.34	2.46	2.41	2.24	2.19	2.41	2.05	2.49	2.42	2.71	2.44	2.35	
$\text{Al}_9^- (\text{C}_1)$	2.11	2.56	2.49	2.43	2.58	2.52	2.36	2.31	2.50	2.10	2.57	2.50	2.82	2.53	2.46	
$\text{Al}_{10}^- (\text{C}_i)$	2.12	2.58	2.52	2.46	2.58	2.52	2.40	2.32	2.52	2.10	2.59	2.52	2.85	2.55	2.47	
$D_e (\text{eV})$																
$\text{Al}_5^- (\text{C}_s)$	2.23	2.58	2.52	2.46	3.51	2.54	2.41	2.35	2.51	2.22	2.65	2.57	2.84	2.55	2.48	
$\text{Al}_6^- (\text{D}_{3d})$	2.66	3.76	3.50	3.38	3.54	3.69	3.36	3.19	3.52	2.57	3.53	3.40	4.13	3.53	3.43	
$\text{Al}_7^- (\text{C}_{3v})$	2.59	3.18	3.05	2.98	3.21	3.12	3.04	2.95	3.05	2.52	3.10	3.00	3.47	3.07	3.11	
$\text{Al}_8^- (\text{C}_{2h})$	1.91	2.21	2.29	2.24	2.11	2.03	1.88	1.81	2.31	1.93	2.39	2.34	2.55	2.35	2.06	
$\text{Al}_9^- (\text{C}_1)$	2.62	3.46	3.24	3.14	3.57	3.43	3.33	3.26	3.23	2.52	3.28	3.16	3.73	3.24	3.36	
$\text{Al}_{10}^- (\text{C}_i)$	2.21	2.74	2.76	2.70	2.58	2.51	2.72	2.50	2.77	2.10	2.73	2.65	3.12	2.76	2.54	

^aValues were calculated by CCSD(T)/def2-QZVPP//PBE0/def2-TZVPP in this work. ^bReference S4. ^cReference S5.

M06, M06-2X, and TPSSh give comparable results (MAE of ~ 0.015 Å for Al_2 – Al_4 clusters; Figure 3a). Their counterpart GGA or meta-GGA DFT functionals, except M06-L, also give good results for predicting the molecular structures of neutral Al clusters; almost no difference between the hybrid (hybrid-meta) and GGA (meta-GGA) is observed. In particular, the TPSS functional shows slightly better performance than other DFT functionals except ω B97XD. This can explain why TPSS was used in previous studies²³ of Al clusters. As shown in Figure 3a, the BLYP functional gives the worst performance for the prediction of neutral cluster structures. The B3LYP functional, which is a hybrid version of BLYP, also shows poor performance. Therefore, BLYP, B3LYP, and M06-L functionals are not recommended for predicting the molecular structures of neutral Al clusters.

Compared to neutral clusters, the B3LYP functional shows noteworthy results for the Al–Al bond lengths for anionic Al clusters (see Table 2 and Figure 3a). In contrast, the ω B97X and ω B97XD functionals show very poor performance in predicting the molecular structures of anionic Al clusters, even though they provided very good results for neutral Al clusters. PBE0, mPW1PW91, and TPSSh as well as their GGA versions (PBE, mPW1PW91, and TPSS) also provide reasonable calculations of geometrical parameters of the Al_2^- – Al_4^- clusters, as in the case of neutral Al clusters. On the other hand, M06-L and BLYP also show poor performance, as in the case of neutral clusters. In summary, to predict reasonable molecular structures of both neutral and anionic Al clusters, PBE, mPW1PW91, and TPSS functionals as well as their hybrid versions (PBE0, mPW1PW91, and TPSSh) are recommended. In particular, TPSS (meta-GGA) provides the best performance for predicting the structures of both neutral and anionic Al clusters. Therefore, the TPSS functional could be useful for predicting the structures of very large Al clusters.

Vibrational Frequencies. The calculated vibrational frequencies for neutral and anionic Al_2 – Al_4 clusters, along with experimental and high-level theoretical data, are summarized in Table S1 in Supporting Information, and their MAEs are shown in Figure 3b. As shown in Figure 3b, B1B95, PBE0, mPW1PW91, TPSSh, and TPSS functionals show less deviation (ca. 5 – 10 cm^{-1}) than other functionals. On the other hand, B3LYP, BLYP, M06, and M06-2X show large MAEs in both neutral and anionic Al_2 – Al_4 clusters. These results suggest that mixing the exact exchange cannot give improved results in the vibrational frequencies of neutral Al clusters. In this case, selecting the functional itself has significant effects in calculating the vibrational frequencies. Both B3LYP (hybrid) and BLYP (GGA) functionals are a combination of Becke exchange (B88) and Lee–Yang–Parr (LYP) correlation functionals. Both BLYP and B3LYP functionals exhibited poor performance, as shown in Figure 3. M06 and M06-2X are both hybrid-meta functionals. Even M06-L (meta-GGA) gives better performance than those functionals. Therefore, to obtain a reasonable vibrational frequency (and molecular structure) of both neutral and anionic Al clusters, the combination of exchange and correlation functionals is a critical factor in these calculations, regardless of whether they are hybrid or pure DFT functionals.

Energetics. Vertical Ionization and Vertical Electron Detachment Energies. The vIEs for neutral clusters and vEDEs for anionic clusters were calculated with a range of DFT functionals. The calculated results of vIE for Al_2 – Al_4 clusters and vEDE for Al_2^- – Al_4^- clusters are summarized in Tables 1 and 2, respectively. In addition, the calculated results of vIE for

Al_5 – Al_{10} clusters and vEDE for Al_5^- – Al_{10}^- clusters are summarized in Tables 3 and 4, respectively. Although experimental results¹⁶ are available for vIE, the error ranges are too large to assess the DFT functionals (see Tables 1 and 3). Therefore, the vIEs of Al_n clusters ($n = 2$ – 10) were calculated by use of CCSD(T)/def2-QZVPP. To adopt their results as the reference values, CCSD(T)/def2-QZVPP single-point energy calculations were performed for the optimized molecular structures by PBE0/def2-TZVPP and CCSD(T)/def2-QZVPP//PBE0/def2-TZVPP because PBE0 provided reasonable results for the molecular structures. As shown in Tables 1 and 3, the vIEs calculated by CCSD(T) lie in the error range of the experimental values or very close to those values. These systematic high-level calculations, CCSD(T) with a quadruple- ζ quality basis set, of vIE up to Al_{10} were performed for the first time to the best of our knowledge.

The MAEs with respect to CCSD(T) results for vIE and experimental values for vEDE are shown in Figure 4, panels a

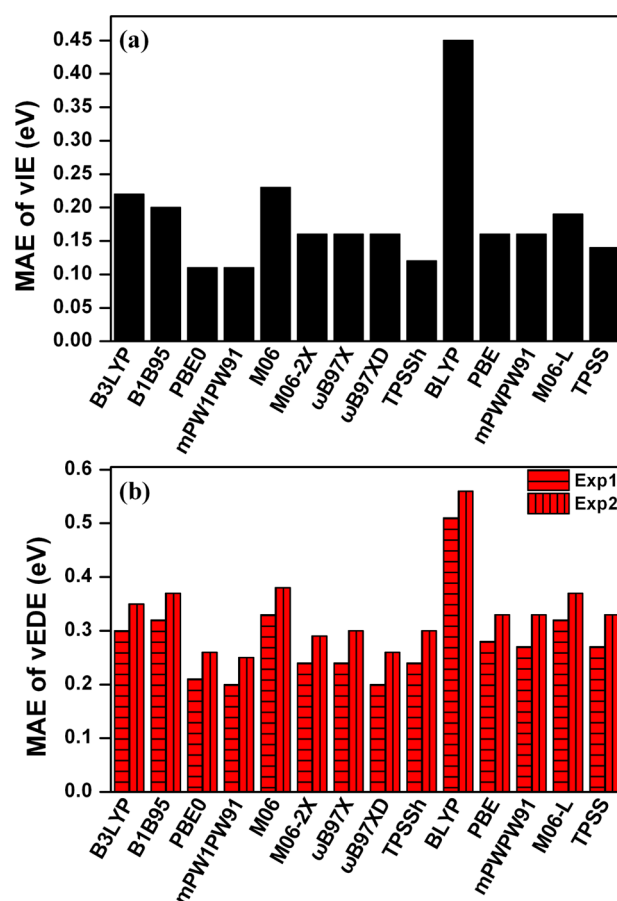


Figure 4. Mean absolute errors of (a) vIE for neutral Al_n ($n = 2$ – 10) clusters and (b) vEDE for anionic Al_n^- ($n = 2$ – 10) clusters. In panel b, Exp1 and 2 refer to values from refs 54 and 55, respectively.

and b, respectively. As shown in Figure 4a, the PBE0 and mPW1PW91 functionals show outstanding results (MAE ~ 0.10 eV) in calculating vIEs, followed by TPSSh. The TPSS functional also provide reasonable results. B3LYP, B1B95, M06, and M06-L functionals show poor performance for the vIE calculations. The deviation is ~ 0.20 eV from the CCSD(T) results. BLYP is the worst method for calculating vIE. Therefore, B3LYP and BLYP are still inappropriate functionals for vIE calculations. In the case of vIE calculation, the

superiority of the hybrid DFT functional has not been observed, as in the calculations of molecular structures and vibrational frequencies.

In vIE calculations, the sharp decrease in vIE on Al_7 is well-known due to the shell structure of Al_7 .²⁵ Indeed, the results of CCSD(T)/def2-QZVPP show the minimum value of vIE on Al_7 . In addition, a recent quantum Monte Carlo (QMC) study also reported sharp minimum behavior in the vIE of Al_n calculations.⁵³ On the other hand, no DFT functionals used in this study give the minimum value of vIE on Al_7 . All DFT functionals except B3LYP show that the vIE of Al_{10} is the minimum for clusters ranging from Al_2 to Al_{10} . The source of this discrepancy is unclear at the moment, but all DFTs might overstabilize Al_{10}^+ , resulting in the smallest vIE on Al_{10} .

As shown in Figure 4b, PBE0 and mPW1PW91 provide results similar to the experimental results,^{54,55} the differences are approximately 0.15–0.25 eV (see Tables 2 and 4). BLYP is still the worst functional for vEDE calculations. A comparison of Figure 4 panels a and b shows that although all MAEs of vEDE are larger than those of vIE, the trend of MAEs (that is, the shape of the histograms) is similar. Therefore, the calculations of vIE also show good performance for calculating vEDE. Therefore, PBE0 and mPW1PW91 are recommended for calculating vIE and vEDE, but the BLYP is an inappropriate functional for calculating vIE and vEDE of Al clusters.

Cohesive and Dissociation Energies. No experimental results are available for E_{coh} and D_e of large neutral and anion clusters. Therefore, E_{coh} and D_e of neutral Al clusters calculated by DFT are compared with those of CCSD(T)/def2-QZVPP.²³ Similarly, the E_{coh} and D_e of anionic Al clusters were calculated by use of CCSD(T)/def2-QZVPP//PBE0/def2-TZVPP for comparison. Calculated results for neutral and anionic Al_2 – Al_4 clusters are summarized in Tables 1 and 2, respectively, and E_{coh} and D_e results for neutral and anionic Al_5 – Al_{10} clusters are summarized in Tables 3 and 4, respectively. MAEs of E_{coh} and D_e with respect to the CCSD(T) values are shown in Figure 5 panels a and b, respectively. E_{coh} values calculated by PBE0, mPW1PW91, and TPSSh are in excellent agreement with the CCSD(T) results for neutral and anionic Al clusters; the deviations are negligible (~ 0.05 eV). The B1B95, M06-2X, mPWPW91, and TPSS functionals also provide reasonable results. On the other hand, large deviations from CCSD(T) values are observed in the B3LYP, BLYP, and M06-L calculations for both neutral and anionic Al clusters. The inferiority of B3LYP for calculating E_{coh} was also shown in a previous study.²³

A comparison of Figure 5 panels a and b shows that the MAEs of D_e exhibit a similar trend to that of E_{coh} . The B3LYP, BLYP, and M06-L functionals show the worst performances. Drebov and Ahlrichs²³ reported that D_e values calculated by TPSS were in close agreement with those of CCSD(T). The maximum absolute deviation of D_e was only 0.15 eV. Similar results are also obtained in this study. No DFT functional that gives dramatically better performance for calculating D_e is observed. B1B95, PBE0, mPW1PW91, M06, TPSSh, PBE, and mPWPW91 give results comparable with those of TPSS in the calculations of D_e ; all MAEs are near 0.1 eV. This error estimation has already been reported in the earlier DFT study (PBE/def2-TZVP) of Al clusters. Our results are also consistent with those of the earlier work.¹¹ The long-range-corrected functionals, ωB97X and ωB97XD , show larger deviations in E_{coh} and D_e than other functionals except B3LYP, BLYP, and M06-L. In the calculations of E_{coh} and D_e ,

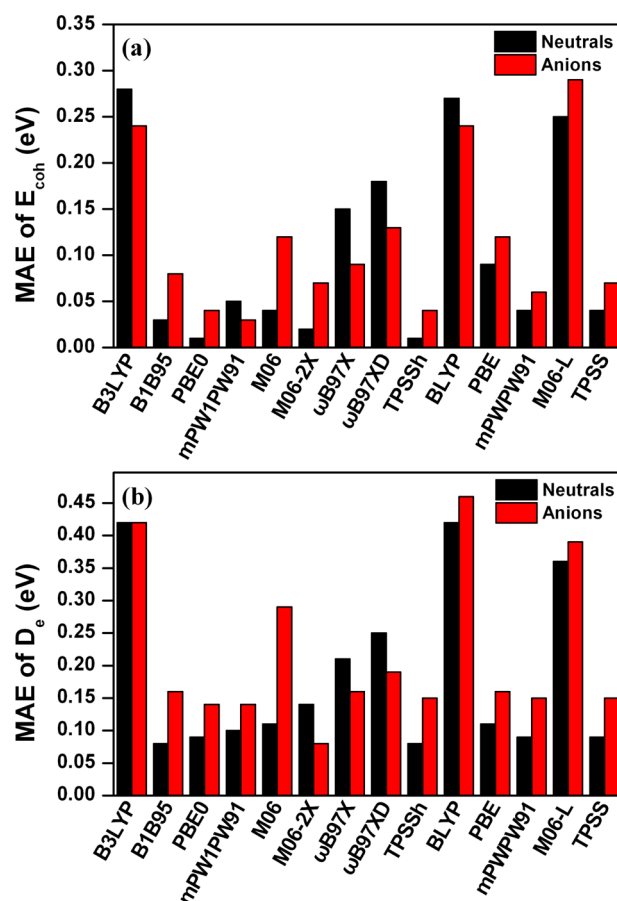


Figure 5. MAE of (a) E_{coh} and (b) D_e from CCSD(T)/def2-QZVPP values for neutral and anionic Al_n ($n = 2$ – 10) clusters.

mixing exact exchange viz. hybrid functionals do not improve the results for E_{coh} and D_e , as was observed in the case of the structure and vibrational frequency.

General Performance. Both BLYP and B3LYP functionals showed very poor performances compared to the other DFT functionals. Paier et al.⁵⁶ reported that the B3LYP functional failed to predict accurate values of energetic parameters, such as the atomization energy and reaction energies of free-electron-like systems, such as metals and semiconductors. In general, the valence electrons of Al have free-electron-like behavior, and the stabilities of small Al_n clusters have been studied by use of a simple jellium model. Therefore, it is understandable that the B3LYP (and also BLYP) functional seriously underestimates the energetic parameters (see Tables 3 and 4). Overall, the PBE0 and mPW1PW91 functionals are recommended for calculating all the molecular properties of neutral and anionic Al clusters. This study is consistent with earlier studies by Schultz et al.²² and Miller et al.,⁵⁷ who suggested that PBE0 performed well in a study of Al clusters. They found small absolute error differences from the results of the PBE0 functional compared to the available experimental results. On the other hand, results calculated with the TPSS functional are also reasonable in terms of cost effectiveness because of less computation time compared to hybrid functionals. Therefore, when calculating larger Al clusters or QM/MD simulations for the catalytic reactions of Al clusters, TPSS with a combination of reasonably sized basis sets is a suitable method.

CONCLUSION

This study assessed the performance of hybrid (B3LYP, PBE0, and mPW1PW91), hybrid-meta (B1B95, M06, M06-2X, and TPSSH), long-range-corrected (ω B97X and ω B97XD), meta-GGA (M06-L and TPSS), and GGA (BLYP, PBE, and mPWPW91) functionals for neutral and anionic Al clusters. Structural and energetic parameters were calculated for neutral and anionic Al_n ($n = 2-10$) clusters by a variety of DFT methods. The PBE, mPWPW91, and TPSS functionals, along with their hybrid functionals PBE0, mPW1PW91, and TPSSH, perform well in the geometry optimizations and vibrational frequency calculations. Therefore, these functionals are recommended for studying the molecular structures and vibrational frequencies of Al clusters. Similarly, PBE0 and mPW1PW91 performed consistently compared to high-level theoretical data and available experimental results for energetic parameters ($v\text{IE}$, $v\text{EDE}$, E_{coh} , and D_e). Generally, B3LYP, which is the most widely used functional, and BLYP show very poor performance for both neutral and anionic clusters, particularly regarding the energetic parameters. The M06 family functionals give poor performances for the overall molecular properties. Overall, the hybrid functionals PBE0 and mPW1PW91 are recommended for examining the structural and energetic parameters of Al clusters. In particular, TPSS (meta-GGA) is recommended for further studies of very large Al clusters. On the other hand, B3LYP, BLYP, and M06-L are not recommended for calculations of Al_n clusters.

ASSOCIATED CONTENT

Supporting Information

One table listing calculated vibrational frequencies of neutral and anionic Al_n ($n = 2-4$) clusters. This material is available free of charge via the Internet at <http://pubs.acs.org>.

AUTHOR INFORMATION

Corresponding Authors

*(J.K.) E-mail: joonghankim@catholic.ac.kr.

*(T.K.K.) E-mail: tkkim@pusan.ac.kr.

Notes

The authors declare no competing financial interest.

ACKNOWLEDGMENTS

This work was supported by National Research Foundation of Korea (NRF) grants funded by the Korean government (MEST and MSIP) (2007-0056095, and NRF-2013R1A1A2009575). T.K.K. also gratefully acknowledges supports by the framework of international cooperation program by NRF of Korea (NRF-2012K2A1A2033072). This research was also supported in part by the Global Research Laboratory Program (Grant 2009-00439), the Leading Foreign Research Institute Recruitment Program (Grant 2010-00471), and the Max Planck POSTECH/Korea Research Initiative Program (Grant 2011-0031558) through NRF funded by Ministry of Science, ICT & Future Planning.

REFERENCES

(1) Ehrlich, R.; Young, A. R.; Rice, G.; Dvorak, J.; Shapiro, P.; Smith, H. F. The Chemistry of Alane. XI. A New Complex Lithium Aluminum Hydride, Li_3AlH_6 . *J. Am. Chem. Soc.* **1966**, *88*, 858–860.
(2) Bazyn, T.; Krier, H.; Glumac, N.; Shankar, N.; Wang, X.; Jackson, T. L. Decomposition of Aluminum Hydride under Solid Rocket Motor Conditions. *J. Prop. Power* **2007**, *23*, 457–464.

(3) Trost, J.; Brune, H.; Wintterlin, J.; Behm, R. J.; Ertl, G. Interaction of Oxygen with $\text{Al}(111)$ at Elevated Temperatures. *J. Chem. Phys.* **1998**, *108*, 1740–1747.
(4) Burgert, R.; Schnockel, H.; Grubisic, A.; Li, X.; Stokes, S. T.; Bowen, K. H.; Gantefor, G. F.; Kiran, B.; Jena, P. Spin Conservation Accounts for Aluminum Cluster Anion Reactivity Pattern with O_2 . *Science* **2008**, *319*, 438–442.
(5) Sunil, K. K.; Jordan, K. D. Determination of the Energies and Spectroscopic Constants of the Low-Lying Electronic States of Al_2 , Al_2^+ , and Al_2^- . *J. Phys. Chem.* **1988**, *92*, 2774–2781.
(6) Jones, R. O. Simulated Annealing Study of Neutral and Charged Clusters: Al_n and Ga_n . *J. Chem. Phys.* **1993**, *99*, 1194–1206.
(7) Yang, S. H.; Drabold, D. A.; Adams, J. B.; Sachdev, A. First-Principles Local-Orbital Density-Functional Study of Al Clusters. *Phys. Rev. B* **1993**, *47*, 1567–1576.
(8) Ahlrichs, R.; Elliott, S. D. Clusters of Aluminium, A Density Functional Study. *Phys. Chem. Chem. Phys.* **1999**, *1*, 13–21.
(9) Rao, B. K.; Jena, P. Evolution of the Electronic Structure and Properties of Neutral and Charged Aluminum Clusters: A Comprehensive Analysis. *J. Chem. Phys.* **1999**, *111*, 1890–1904.
(10) Bergeron, D. E.; Castleman, A. W.; Morisato, T.; Khanna, S. N. Formation of Al_{13}^- : Evidence for the Superhalogen Character of Al_{13} . *Science* **2004**, *304*, 84–87.
(11) Drebov, N.; Ahlrichs, R. Structures of Al_n , Its Anions and Cations up to $n = 34$: A Theoretical Investigation. *J. Chem. Phys.* **2010**, *132*, No. 164703.
(12) Wang, C. J.; Kuang, X. Y.; Wang, H. Q.; Li, H. F.; Mao, A. J. Geometries, Stabilities, Electronic, and Magnetic Properties of Small Aluminum Cluster Anions Doped with Iron: A Density Functional Theory Study. *Comput. Theor. Chem.* **2012**, *980*, 7–14.
(13) Datta, A.; Pati, S. K. Charge-Transfer Induced Large Nonlinear Optical Properties of Small Al Clusters: Al_4M_4 ($M = \text{Li}, \text{Na}, \text{and K}$). *J. Phys. Chem. A* **2004**, *108*, 9527–9530.
(14) Kim, J. C.; Kim, K. H.; Jung, J.; Han, Y. K. Reaction Mechanisms of Dissociative Chemisorption of HI , I_2 , and CH_3I on a Magic Cluster Al_{13}^- . *J. Comput. Chem.* **2008**, *29*, 1626–1631.
(15) Cox, D. M.; Trevor, D. J.; Whetten, R. L.; Rohlfing, E. A.; Kaldor, A. Aluminum Clusters: Magnetic Properties. *J. Chem. Phys.* **1986**, *84*, 4651–4656.
(16) Cox, D. M.; Trevor, D. J.; Whetten, R. L.; Kaldor, A. Aluminum Clusters: Ionization Thresholds and Reactivity toward Deuterium, Water, Oxygen, Methanol, Methane and Carbon Monoxide. *J. Phys. Chem.* **1988**, *92*, 421–429.
(17) Cooper, B. T.; Parent, D.; Buckner, S. W. Oxidation Reactions and Photochemistry of Aluminum Cluster Anions (Al_3^- to Al_{23}^-). *Chem. Phys. Lett.* **1998**, *284*, 401–406.
(18) Hettich, R. L. Structural Investigations of Aluminum Cluster Ions, Al_n^- ($n = 3-50$). *J. Am. Chem. Soc.* **1989**, *111*, 8582–8588.
(19) Han, Y. K.; Jung, J. H.; Kim, K. H. Structure and Stability of Al_{13}H Clusters. *J. Chem. Phys.* **2005**, *122*, 124319.
(20) Schultz, N. E.; Truhlar, D. G. New Effective Core Method (Effective Core Potential and Valence Basis Set) for Al Clusters and Nanoparticles and Heteronuclear Al-Containing Molecules. *J. Chem. Theory Comput.* **2005**, *1*, 41–53.
(21) Henry, D. J.; Varano, A.; Yarovsky, I. Performance of Numerical Basis Set DFT for Aluminum Clusters. *J. Phys. Chem. A* **2008**, *112*, 9835–9844.
(22) Schultz, N. E.; Staszewska, G.; Staszewski, P.; Truhlar, D. G. Validation of Theoretical Methods for the Structure and Energy of Aluminum Clusters. *J. Phys. Chem. B* **2004**, *108*, 4850–4861.
(23) Drebov, N.; Ahlrichs, R. Small Clusters of Aluminum and Tin: Highly Correlated Calculations and Validation of Density Functional Procedures. *J. Chem. Phys.* **2011**, *134*, No. 124308.
(24) Pino, I.; Kroes, G. J.; van Hemert, M. C. Hydrogen Dissociation on Small Aluminum Clusters. *J. Chem. Phys.* **2010**, *133*, No. 184304.
(25) Sun, J.; Lu, W. C.; Wang, H.; Li, Z. S.; Sun, C. C. Theoretical Study of Al_n and Al_nO ($n = 2-10$) Clusters. *J. Phys. Chem. A* **2006**, *110*, 2729–2738.

- (26) Geske, G. D.; Boldyrev, A. I.; Li, X.; Wang, L. S. On the Origin of Planarity in Al_5^- and Al_5 Clusters: The Importance of a Four-Center Peripheral Bond. *J. Chem. Phys.* **2000**, *113*, 5130–5133.
- (27) Alexandrou, E. I.; Gross, A.; Bacalis, N. C. Theoretical Investigation of the Interaction of CH_4 with Al_2 and Al_3 Neutral and Charged Clusters. *J. Chem. Phys.* **2010**, *132*, No. 154701.
- (28) Bacalis, N. C.; Metropoulos, A.; Gross, A. Theoretical Study of the $\text{O}_2 + \text{Al}_4$ (Tetrahedral) System in Its Singlet State and Comparisons with Its Triplet State. *J. Phys. Chem. C* **2012**, *116*, 16430–16435.
- (29) Becke, A. D. Density-Functional Exchange-Energy Approximation with Correct Asymptotic Behavior. *Phys. Rev. A* **1988**, *38*, 3098–3100.
- (30) Lee, C. T.; Yang, W. T.; Parr, R. G. Development of the Colle-Salvetti Correlation-Energy Formula into a Functional of the Electron Density. *Phys. Rev. B* **1988**, *37*, 785–789.
- (31) Becke, A. D. Density-Functional Thermochemistry. IV. A New Dynamical Correlation Functional and Implications for Exact-Exchange Mixing. *J. Chem. Phys.* **1996**, *104*, 1040–1046.
- (32) Adamo, C.; Barone, V. Toward Reliable Density Functional Methods without Adjustable Parameters: The PBE0 Model. *J. Chem. Phys.* **1999**, *110*, 6158–6170.
- (33) Adamo, C.; Barone, V. Exchange Functionals with Improved Long-Range Behavior and Adiabatic Connection Methods without Adjustable Parameters: The mPW and mPW1PW Models. *J. Chem. Phys.* **1998**, *108*, 664–675.
- (34) Perdew, J. P. *Electronic Structure of Solids*. Akademik Verlag: Berlin, Germany, 1991.
- (35) Zhao, Y.; Truhlar, D. G. The M06 Suite of Density Functionals for Main Group Thermochemistry, Thermochemical Kinetics, Non-covalent Interactions, Excited States, and Transition Elements: Two New Functionals and Systematic Testing of Four M06-Class Functionals and 12 Other Functionals. *Theor. Chem. Acc.* **2008**, *120*, 215–241.
- (36) Chai, J. D.; Head-Gordon, M. Systematic Optimization of Long-Range Corrected Hybrid Density Functionals. *J. Chem. Phys.* **2008**, *128*, No. 084106.
- (37) Chai, J. D.; Head-Gordon, M. Long-Range Corrected Hybrid Density Functionals with Damped Atom-Atom Dispersion Corrections. *Phys. Chem. Chem. Phys.* **2008**, *10*, 6615–6620.
- (38) Staroverov, V. N.; Scuseria, G. E.; Tao, J. M.; Perdew, J. P. Comparative Assessment of a New Nonempirical Density Functional: Molecules and Hydrogen-Bonded Complexes. *J. Chem. Phys.* **2003**, *119*, 12129–12137.
- (39) Perdew, J. P.; Burke, K.; Ernzerhof, M. Generalized Gradient Approximation Made Simple. *Phys. Rev. Lett.* **1996**, *77*, 3865–3868.
- (40) Perdew, J. P.; Ernzerhof, M.; Burke, K. Rationale for Mixing Exact Exchange with Density Functional Approximations. *J. Chem. Phys.* **1996**, *105*, 9982–9985.
- (41) Zhao, Y.; Truhlar, D. G. A New Local Density Functional for Main-Group Thermochemistry, Transition Metal Bonding, Thermochemical Kinetics, and Noncovalent Interactions. *J. Chem. Phys.* **2006**, *125*, No. 194101.
- (42) Tao, J.; Perdew, J. P.; Staroverov, V. N.; Scuseria, G. E. Climbing the Density Functional Ladder: Nonempirical Meta-Generalized Gradient Approximation Designed for Molecules and Solids. *Phys. Rev. Lett.* **2003**, *91*, No. 146401.
- (43) Weigend, F.; Ahlrichs, R. Balanced Basis Sets of Split Valence, Triple Zeta Valence and Quadruple Zeta Valence Quality for H to Rn: Design and Assessment of Accuracy. *Phys. Chem. Chem. Phys.* **2005**, *7*, 3297–3305.
- (44) Raghavachari, K.; Trucks, G. W.; Pople, J. A.; Head-Gordon, M. A Fifth-Order Perturbation Comparison of Electron Correlation Theories. *Chem. Phys. Lett.* **1989**, *157*, 479–483.
- (45) Fournier, R. Trends in Energies and Geometric Structures of Neutral and Charged Aluminum Clusters. *J. Chem. Theory Comput.* **2007**, *3*, 921–929.
- (46) Frisch, M. J.; Trucks, G. W.; Schlegel, H. B.; Scuseria, G. E.; Robb, M. A.; Cheeseman, J. R.; Scalmani, G.; Barone, V.; Mennucci, B.; Petersson, G. A.; Nakatsuji, H.; Caricato, M.; Li, X.; Hratchian, H. P.; Izmaylov, A. F.; Bloino, J.; Zheng, G.; Sonnenberg, J. L.; Hada, M.; Ehara, M.; Toyota, K.; Fukuda, R.; Hasegawa, J.; Ishida, M.; Nakajima, T.; Honda, Y.; Kitao, O.; Nakai, H.; Vreven, T.; Montgomery, J. A., Jr.; Peralta, J. E.; Ogliaro, F.; Bearpark, M.; Heyd, J. J.; Brothers, E.; Kudin, K. N.; Staroverov, V. N.; Kobayashi, R.; Normand, J.; Raghavachari, K.; Rendell, A.; Burant, J. C.; Iyengar, S. S.; Tomasi, J.; Cossi, M.; Rega, N.; Millam, N. J.; Klene, M.; Knox, J. E.; Cross, J. B.; Bakken, V.; Adamo, C.; Jaramillo, J.; Gomperts, R.; Stratmann, R. E.; Yazyev, O.; Austin, A. J.; Cammi, R.; Pomelli, C.; Ochterski, J. W.; Martin, R. L.; Morokuma, K.; Zakrzewski, V. G.; Voth, G. A.; Salvador, P.; Dannenberg, J. J.; Dapprich, S.; Daniels, A. D.; Farkas, Ö.; Foresman, J. B.; Ortiz, J. V.; Cioslowski, J.; Fox, D. J. *Gaussian 09, Revision D.01*; Gaussian Inc., Wallingford, CT, 2009.
- (47) Fu, Z.; Lemire, G. W.; Bishea, G. A.; Morse, M. D. Spectroscopy and Electronic Structure of Jet-Cooled Al_2 . *J. Chem. Phys.* **1990**, *93*, 8420–8441.
- (48) Cai, M. F.; Dzugas, T. P.; Bondybey, V. E. Fluorescence Studies of Laser Vaporized Aluminum: Evidence for a $^3\Pi_u$ Ground State of Aluminum Dimer. *Chem. Phys. Lett.* **1989**, *155*, 430–436.
- (49) Villalta, P. W.; Leopold, D. G. A Study of the Ground and Excited States of Al_3 and Al_3^- . I. 488 nm Anion Photoelectron Spectrum. *J. Chem. Phys.* **2009**, *130*, No. 024303.
- (50) Fu, Z. W.; Lemire, G. W.; Hamrick, Y. M.; Taylor, S.; Shui, J. C.; Morse, M. D. Spectroscopic Studies of the Jet-Cooled Aluminum Trimer. *J. Chem. Phys.* **1988**, *88*, 3524–3531.
- (51) Czernek, J.; Živný, O. The MRCI Studies of Low-Lying Electronic States of Al_3 and Al_3^- . *Chem. Phys. Lett.* **2011**, *512*, 40–43.
- (52) Zhan, C. G.; Zheng, F.; Dixon, D. A. Electron Affinities of Al_n Clusters and Multiple-Fold Aromaticity of the Square Al_4^{2-} Structure. *J. Am. Chem. Soc.* **2002**, *124*, 14795–14803.
- (53) Candido, L.; Rabelo, J. N. T.; Da Silva, J. L. F.; Hai, G. Q. Quantum Monte Carlo Study of Small Aluminum Clusters Al_n ($n = 2-13$). *Phys. Rev. B* **2012**, *85*, No. 245404.
- (54) Li, X.; Wu, H.; Wang, X.-B.; Wang, L.-S. $s-p$ Hybridization and Electron Shell Structures in Aluminum Clusters: A Photoelectron Spectroscopy Study. *Phys. Rev. Lett.* **1998**, *81*, 1909–1912.
- (55) Cha, C. Y.; Gantefor, G.; Eberhardt, W. The Development of the 3p and 4p Valence Band of Small Aluminum and Gallium Clusters. *J. Chem. Phys.* **1994**, *100*, 995–1010.
- (56) Paier, J.; Marsman, M.; Kresse, G. Why Does the B3LYP Hybrid Functional Fail for Metals? *J. Chem. Phys.* **2007**, *127*, No. 024103.
- (57) Miller, S. R.; Schultz, N. E.; Truhlar, D. G.; Leopold, D. G. A Study of the Ground and Excited States of Al_3 and Al_3^- . II. Computational Analysis of the 488 nm Anion Photoelectron Spectrum and a Reconsideration of the Al_3 Bond Dissociation Energy. *J. Chem. Phys.* **2009**, *130*, No. 024304.